Available online at www.sciencedirect.com
SCIENCE DIRECT®
Journal of Electron Spectroscopy and Related Phenomena 151 (2006) 92–96
JOURNAL OF ELECTRON SPECTROSCOPY and Related Phenomena
www.elsevier.com/locate/elspec

An investigation of distorted wave effects in π^* like molecular orbital by electron momentum spectroscopy

X.G. Ren, C.G. Ning, J.K. Deng*, S.F. Zhang, G.L. Su, Y.R. Huang, G.Q. Li

Department of Physics and Key Laboratory of Atomic and Molecular NanoSciences of MOE, Tsinghua University, Beijing 100084, PR China

Received 19 October 2005; received in revised form 8 November 2005; accepted 8 November 2005
Available online 13 December 2005

Abstract

Sensitive images of orbital electron density for the ethane (C_2H_6) were investigated by using a newly developed electron momentum spectrometer with a wide range of experimental impact energies. Some 'turn up' effects in the momentum distributions of the $1E_g$ and $3A_{1g}$ orbitals were observed at low and high momentum regions compared with plane wave impulse approximation calculations. Moreover, such discrepancies become smaller with the increase in the impact electron energy. The distorted wave effects could be a reasonable explanation for these observed discrepancies. While appropriate theoretical calculations using distorted wave in molecules could not be achieved at present.

Keywords: Electron momentum spectroscopy; Distorted wave effects; Ethane

1. Introduction

Electron momentum spectroscopy (EMS), also known as binary (e, 2e) spectroscopy, is a kinematically complete ionization process. As a powerful probe it can effectively image orbital electron density and provide direct information on the nature of electron transfer processes [1–4]. As such, EMS can provide new insights into understanding and predicting physical and chemical behavior at the fundamental electronic level. Recently, a high performance (e, 2e) electron momentum spectrometer in the symmetric noncoplanar geometry with simultaneous detection in energy and momentum has been developed at Tsinghua University [5]. In this (e, 2e) electron impact ionization experiment a novel double toroidal analyzer (DTA) and a pair of wedge strip anode (WSA) position sensitive detectors (PSDs) with a USB muti-parameters data-acquisition system [6] were used. The typical energy and coincidence time resolution of 1.2 eV and 2 ns, the θ and ϕ angle resolution of $\pm 0.7^\circ$ and $\pm 1.9^\circ$ were achieved with the EMS measurements of argon and helium [5].

With the EMS spectrometer performance improvements in energy and angle resolutions, detection sensitivity, coincidence counting rate and experimental stability, many fresh and valuable experiments, such as the EMS studies in the more complex systems, cluster, self-ionization and excitation–ionization, and the dilute target systems, are feasible within a practical length of time. Furthermore, the high performance measurements at a wide range of impact electron energies in the present spectrometer has made it possible for the systematical investigations of the distorted wave effects in molecules [4,7], which require a wide range of experimental impact energies and is difficult for the previous EMS spectrometers [7].

In this work, the 'turn up' effects occurred at low and high momentum region of momentum distributions in the ethane π^* like orbital were observed with the (e, 2e) reaction at the impact energies of 400, 600, 800, 1000, 1200 and 1600 eV. The imaging of orbital electron density distributions were directly obtained by using our new EMS spectrometer with simultaneous detection in energy and momentum. The theoretical calculations were carried out using the plane wave impulse approximation (PWIA), while the molecular distorted wave (DW) theory could not be achieved due to the multi-centre nature for molecule targets, which is another main motivation for the convincingly investigating the molecular distorted wave effects.

2. Experimental details and reaction theory

In our EMS experiment an incident electron of energy E_0 causes the ionization of the target system and the scattered

* Corresponding author. Tel.: +86 10 6278 5594; fax: +86 10 6278 1604.
E-mail address: djk-dmp@tsinghua.edu.cn (J.K. Deng).

0368-2048/$ – see front matter © 2005 Elsevier B.V. All rights reserved.
doi:10.1016/j.elspec.2005.11.003

and ionized electrons are subsequently detected in coincidence at the same kinetic energies and the same polar angles, i.e. $E_1 \approx E_2$, and $\theta_1 = \theta_2 = 45^\circ$. In this kinematic arrangement the ionized electron essentially undergoes a clean 'knock out' collision, and the distorted wave impulse approximation (DWIA) and PWIA can provide a description of the collision, respectively [3,8,9]. The (e, 2e) cross-section for randomly oriented targets is given by:

$$\sigma_{(e,2e)} = 2\pi^4 \frac{\vec{p}_1\vec{p}_2}{\vec{p}_0}\sigma_{\text{Mott}} \times \int d\Omega \left| \left\langle \chi^{(-)}(\vec{p}_1)\chi^{(-)}(\vec{p}_2)\Psi_f^{N-1} \left| \Psi_i^N \chi^{(+)}(\vec{p}_0) \right\rangle \right|^2 \quad (1)$$

within DWIA, or

$$\sigma_{(e,2e)} = 2\pi^4 \frac{\vec{p}_1\vec{p}_2}{\vec{p}_0}\sigma_{\text{Mott}} \times \int d\Omega \left| \left\langle \vec{p}\Psi_f^{N-1} \left| \Psi_i^N \right\rangle \right|^2 \quad (2)$$

within PWIA. Where σ_{Mott} is the Mott scattering cross-section. $\left|\Psi_f^{N-1}\right\rangle$ and $\left|\Psi_i^N\right\rangle$ are the total electronic wave functions for the final ion state and the target molecule ground (initial) state, respectively. And $\vec{p}_0$, $\vec{p}_1$, $\vec{p}_2$ and $\vec{p}$ are the momentum for the incident, the two outgoing and the target orbital (ionized) electrons, respectively. The spherical averaging $\int d\Omega$ is due to the random orientation of gaseous targets. In DWIA the motion of the external electrons is represented by elastic-scattering functions, calculated in a distorted potential. $\chi^{(-)}(\vec{p}_1)$, $\chi^{(-)}(\vec{p}_2)$ and $\chi^{(+)}(\vec{p}_0)$ are distorted waves for the two outgoing and incoming electrons, respectively. In PWIA the distortion effects on the electron waves are negligible, and the electron waves are replaced by plane waves. The overlap of the ion and neutral wave functions in Eq. (2) is known as Dyson orbital.

Within the PWIA, the target Hartree–Fock approximation (THFA) [3,10] and target Kohn–Sham approximation (TKSA) [10,11] have been proposed as a means of approximating Dyson orbitals by Hartree–Fock (HF) or Kohn–Sham (KS) orbital. Within these further approximations the (e, 2e) cross-sections in Eq. (2) can be reduced to

$$\sigma_{(e,2e)} \propto \int d\Omega \left|\psi_j(p)\right|^2 \quad (3)$$

where $\psi_j(p)$ is the one-electron momentum space canonical HF or KS orbital wave function in the neutral initial state for the jth electron which was ionized.

Theoretical momentum profiles of ethane were calculated using the HF and density functional theory (DFT) methods. Briefly, position–space wave functions of the molecules were generated by using the Gaussian98 program and were subsequently converted to momentum profiles with the HEMS program developed by Brion and his co-workers. To compare with experiment all the theoretical profiles were convoluted with the instrumental momentum resolutions according to the Gaussian method [12].

3. Results and discussion

The typical experimental image of orbital electron density for ethane has been directly obtained and shown in Fig. 1, compared with the theoretical result. The experimental measurement was performed at impact electron energy of 1000 with 100 eV

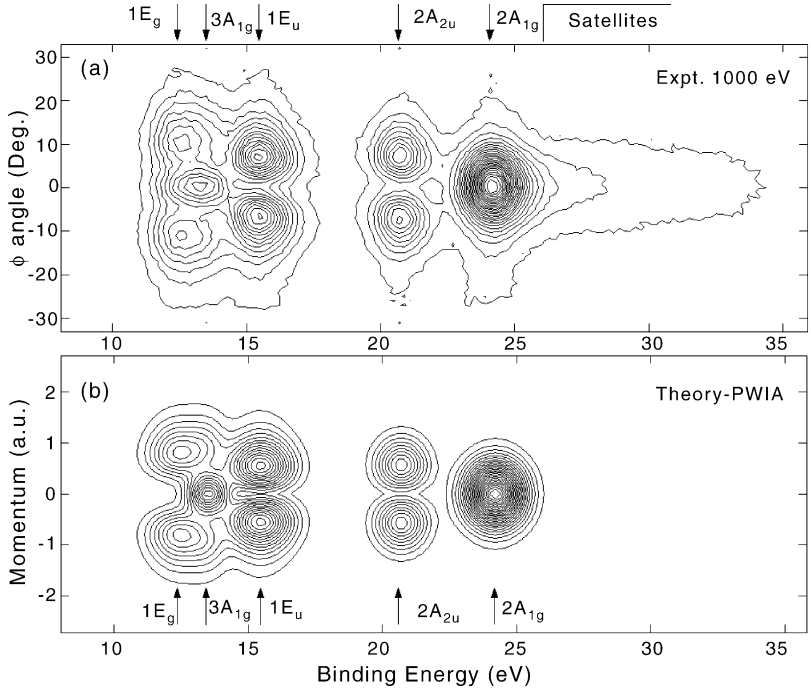

Fig. 1. The contour images of orbital electron densities for ethane. (a) Experimental measurement at the impact-energy of 1000 eV and (b) PWIA calculation with DFT method.

passing energy in the analyzer, as shown in Fig. 1(a). And the theoretical density distribution was calculated by using the DFT method with the B3LYP functional inclusion of the instrumental resolutions, as shown in Fig. 1(b). The contour images represent energy–momentum densities of valence electrons in ethane and contain a wealth of information on relative intensities, momentum distribution, symmetries of the states involved and satellite structures. Our expected orbital electron momentum distributions and binding energy spectra can be directly obtained with this image. From the intensity distribution along the binding energy axis the binding energy spectrum is obtained at different angle ϕ (i.e. electron momentum), which includes the $1E_g$, $3A_{1g}$, $1E_u$, $2A_{2u}$ and $2A_{1g}$ states, as well as the $2A_{1g}$ satellite states. The angle ϕ is the azimuthal angle difference between the two outgoing electrons, and it is also equivalent to the target orbital (ionized) electron momentum p [3,5]. On the other hand, the orbital electron density distribution can be obtained along the ϕ angle axis at a given binding energies region (represent specifically orbital).

Comparing the experimental orbital electron density image (Fig. 1(a)) with the theoretical result (Fig. 1(b)) we can observe somewhat discrepancy at the binding energy region of $1E_g$ and $3A_{1g}$ orbitals. In order to more clearly investigate this discrepancy the experimental and theoretical momentum distributions for the $1E_g$, $3A_{1g}$ and the summed $1E_g$ and $3A_{1g}$ orbitals have been obtained, as shown in Fig. 2. The theoretical momentum distributions were calculated by using THFA and TKSA within PWIA. For comparing with the experimental electron momentum distributions, these theoretical profiles were convoluted with the instrumental resolutions ($\Delta\theta = \pm 0.7^\circ$, $\Delta\phi = \pm 1.9^\circ$, and $\Delta E = 1.2$ eV) with a Gaussian method [12]. The significant "turn up" effects of (e, 2e) cross-section between the experimental data and all of the theoretical predictions of $1E_g$ orbital have been observed in the low and high momentum region, as shown in Fig. 2(a). Similar "turn up" effect has also been observed by Deng et al. [13] at one impact-energy of 1200 eV. Such "turn up" effects (shown as Fig. 2(a)) are possibly due to "contamination" from the neighboring $3A_{1g}$ orbital, which shows an intense "s–p" type distribution as shown in Fig. 2(b). However, this explanation could be negated from the comparison of the summed $1E_g$ and $3A_{1g}$ orbitals momentum distributions between experimental measurement and theoretical calculations shown in Fig. 2(c). There is still a significant "turn up" effect of (e, 2e) cross-section for the summed $1E_g$ and $3A_{1g}$ orbitals, which could be subjected to some particular effects that the current theoretical treatments have not given full consideration, such as the distorted wave effects.

The occurrence of distortion effects of $1E_g$ orbital at higher momentum region can readily be understood since this region of the electron momentum profile involves significant penetration by the incoming electron into the smaller r region, near to the nucleus [3,9,14]. How distortion wave effects could arise at low momentum (p) since such regions of the electron density are normally considered to be located at larger r, i.e. far from the nuclei. In order to more convincingly investigate this "turn up" effect the orbital electron densities of ethane have been measured at different impact electron energies of 400, 600,

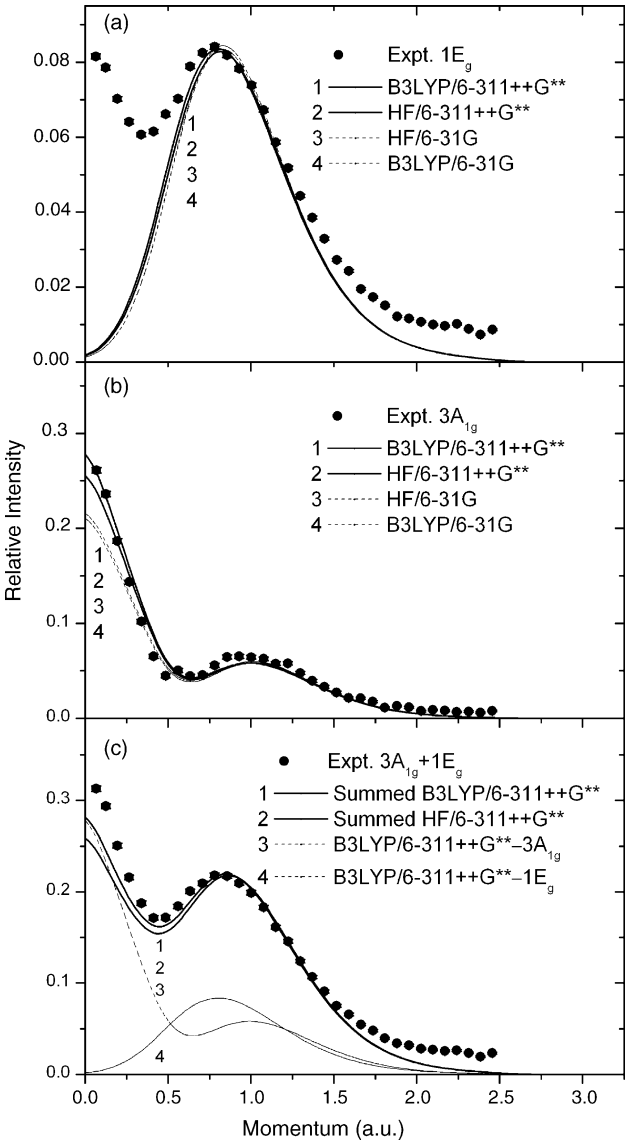

Fig. 2. The experimental and theoretical orbital electron momentum distributions for ethane of (a) $1E_g$ orbital, (b) $3A_{1g}$ orbital and (c) the summed $1E_g$ and $3A_{1g}$ orbitals, obtained at an impact-energy of 1000 eV in EMS experiment, compared with HF and DFT calculations.

800, 1000, 1200 and 1600 eV. The experimental impact-energy dependence of the momentum distributions of the summed $1E_g$ and $3A_{1g}$ orbitals were obtained and shown in Fig. 3 with the theoretical calculations. The significant 'turn up' effects of the (e, 2e) cross-sections compared with the theoretical calculations have also been observed at these different impact electron energies, and more importantly such 'turn up' effects become smaller with the increase in the impact electron energy of the (e, 2e) reaction.

Further consideration of the relative phase in the position space wave function contour image for the $1E_g$ and $3A_{1g}$ orbitals, as shown in Fig. 4, indicates that the $1E_g$ orbital has strong π^* like character. It has been found [4,8,15] that such orbital usually produce a "turn up" of the cross-section in the low momentum region, and this behavior is similar to the low-p effect observed

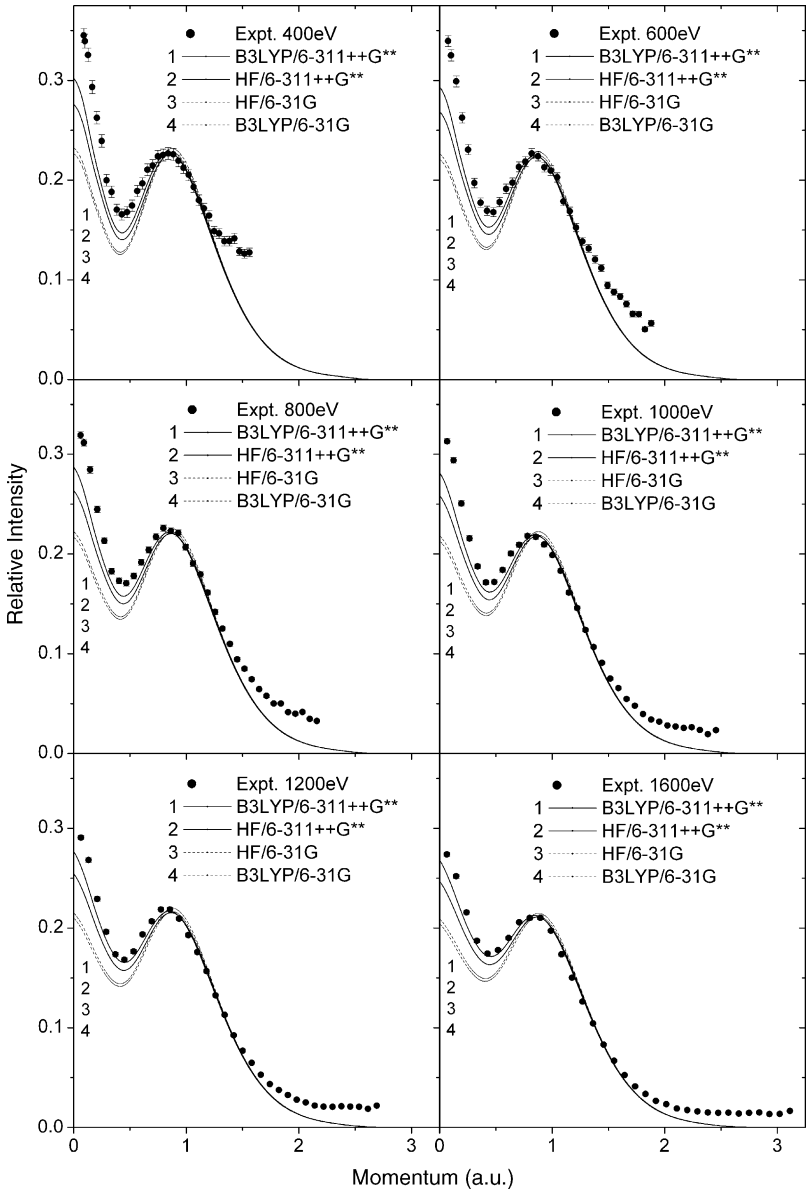

Fig. 3. The experimental momentum distributions of the ethane $1E_g$ and $3A_{1g}$ orbitals at the impact energies of 400, 600, 800, 1000, 1200 and 1600 eV compared with the PWIA calculations.

in atomic *n*d orbitals EMS experiment [8,15]. This situation is also probably the case for the $1E_g$ orbital of ethane. Theoretical studies of atomic targets indicated that such effects in *n*d orbitals are due to breakdown of the PWIA caused by significant low momentum components near the nucleus which can occur in orbitals of gerade symmetry for $l \geq 2$. Distorted wave calculations [8,15] in atomic *n*d orbitals have also theoretically predicted that such effects will diminish with the increase of impact electron energy, which is consistent with the experimental investigations in Fig. 3. Under the *n*d atomic distorted wave calculations and the experimental measurements at different impact energies it could be confirmed that the observed 'turn up' effects in the momentum distributions of $1E_g$ π^* like molecular orbital at low momentum region are due to the distorted wave effect. Unfortunately, at present the distorted wave calculations are only possible for atoms but not for molecules due to the multi-centre nature. However, it could be somewhat satisfied for us that the developments of molecular distorted wave theory will benefit from the sensitive experimental measurements of the π^* like molecular orbital at a wide range of different impact energies. Furthermore, it can be seen from the 1600 eV results of momentum distributions that the 1600 eV impact-energy could be near to the high-energy limit of the PWIA validity for the ethane $1E_g$ orbital. However, for the ethylene $1B_{3g}$ orbital [4] and the other studied targets of He [16], H_2 [17], 1,3-cyclohexadiene [18], glyoxal and biacetyl [19] the validity range of the PWIA were very different. So the energy limit for the impact-energy dependence effects and the validity range of the PWIA could depend on the targets [19].

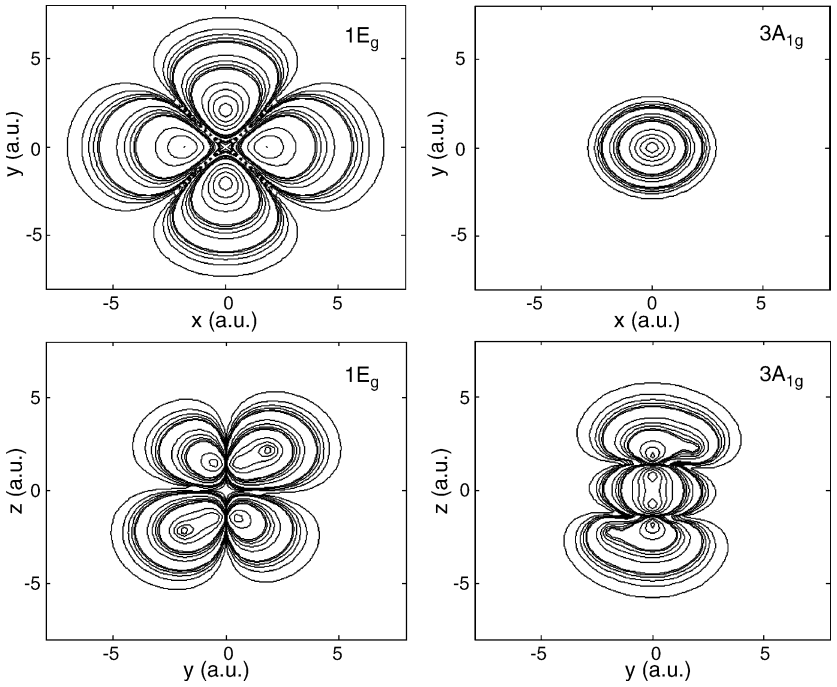

Fig. 4. Position space wave function topograph contour for the $1E_g$ and $3A_{1g}$ orbitals showing that the $1E_g$ orbital has strong π^* like character which is similar to d-type atomic orbital with regard to symmetry.

4. Summary

In summary the study reported the impact-energy dependence of the momentum distributions of the ethane $1E_g$ and $3A_{1g}$ orbitals, measured at different impact energies of 400, 600, 800, 1000, 1200 and 1600 eV with our newly developed EMS spectrometer. The significant 'turn up' effects of (e, 2e) cross-sections in $1E_g$ and the summed $1E_g$ and $3A_{1g}$ orbitals were observed in the low and high *p* region compared with the PWIA theory. Moreover, such observed 'turn up' effects become smaller with the increase in the impact electron energy. It could be confirmed that the observed 'turn up' effects are due to the distorted wave effect of $1E_g$ π^* like molecular orbital under the further considerations of the $1E_g$ and $3A_{1g}$ orbitals wave function character. Besides, the energy limit of the impact-energy dependence effects could be sensitive to the studied targets and orbitals.

Acknowledgements

Project supported by the National Natural Science Foundation of China under Grant nos. 19854002, 19774037 and 10274040 and the Research Fund for the Doctoral Program of Higher Education under Grant no. 1999000327.

References

[1] E. Weigold, I.E. McCarthy, Electron Momentum Spectroscopy, Kulwer Academic/Plenum Publishers, New York, 1999.
[2] C.E. Brion, Int. J. Quantum Chem. 29 (1986) 1397.
[3] I.E. McCarthy, E. Weigold, Rep. Prog. Phys. 54 (1991) 789.
[4] X.G. Ren, C.G. Ning, J.K. Deng, S.F. Zhang, G.L. Su, F. Huang, G.Q. Li, Phys. Rev. Lett. 94 (2005) 163201.
[5] X.G. Ren, C.G. Ning, J.K. Deng, S.F. Zhang, G.L. Su, F. Huang, G.Q. Li, Rev. Sci. Instrum. 76 (2005) 063103.
[6] C.G. Ning, J.K. Deng, G.L. Su, H. Zhou, X.G. Ren, Rev. Sci. Instrum. 75 (2004) 3062.
[7] C.E. Brion, G. Cooper, R. Feng, S. Tixier, Y. Zheng, I.E. McCarthy, Z. Shi, S. Wolfe, Conference Proceedings 604, Correlations, Polarization, and Ionization in Atomic Systems, 2002, p. 38.
[8] C.E. Brion, Y. Zheng, J. Rolke, J.J. Neville, I.E. McCarthy, J. Wang, J. Phys. B 31 (1998) L223.
[9] S. Mazevet, I.E. McCarthy, Y. Zhou, J. Phys. B 29 (1996) L901.
[10] Y. Zheng, J. Rolke, G. Cooper, C.E. Brion, J. Electron Spectrosc. Relat. Phenom. 123 (2002) 377.
[11] P. Duffy, D.P. Chong, M.E. Casida, D.R. Salahub, Phys. Rev. A 50 (1994) 4707.
[12] J.N. Migdall, M.A. Coplan, D.S. Hench, J.H. Moore, J.A. Tossell, V.H. Smith Jr., J.W. Liu, Chem. Phys. 57 (1981) 141.
[13] J.K. Deng, G.Q. Li, X.D. Wang, J.D. Huang, H. Deng, C.G. Ning, Y. Wang, Y. Zheng, J. Chem. Phys. 117 (2002) 4839.
[14] X.G. Ren, C.G. Ning, J.K. Deng, S.F. Zhang, G.L. Su, F. Huang, G.Q. Li, Chem. Phys. Lett. 404 (2005) 279.
[15] M.J. Brunger, S.W. Braidwood, I.E. McCarthy, E. Weigold, J. Phys. B 27 (1994) L597.
[16] X.G. Ren, C.G. Ning, J.K. Deng, G.L. Su, S.F. Zhang, Y.R. Huang, G.Q. Li, Phys. Rev. A 72 (2005) 042718.
[17] M. Takahashi, Y. Khajuria, Y. Udagawa, Phys. Rev. A 68 (2003) 042710.
[18] C.G. Ning, X.G. Ren, J.K. Deng, S.F. Zhang, G.L. Su, F. Huang, G.Q. Li, Chem. Phys. Lett. 407 (2005) 423.
[19] M. Takahashi, T. Saito, J. Hiraka, Y. Udagawa, J. Phys. B 36 (2003) 2539.